J|A|C|S
ARTICLES

Published on Web 09/18/2009

Abrasion as a Catalyst Deposition Technique for Carbon Nanotube Growth

Noe T. Alvarez,[†,‡] Cary L. Pint,[‡,§] Robert H. Hauge,*[,†,‡] and James M. Tour*[,†,‡,||]

Department of Chemistry, Department of Physics and Astronomy, Department of Mechanical Engineering and Materials Science, and The Richard E. Smalley Institute for Nanoscale Science and Technology, Rice University, MS 222, 6100 Main Street, Houston, Texas 77005

Received July 9, 2009; E-mail: hauge@rice.edu; tour@rice.edu

Abstract: Mechanical abrasion of stainless steel (SS) surfaces is demonstrated as an effective technique for the deposition of catalyst to support growth of high density layers of carbon nanotubes (CNTs) in water-assisted catalytic chemical vapor deposition. In all cases of Fe-containing materials abraded on Al_2O_3 substrates, CNT growth is observed; the 400 series of SS appears to deposit catalyst most efficiently. We demonstrate that this simple abrasion technique enables both micro- and nanoscale accuracy in catalyst patterning as well as large area catalyst deposition for uniform, dense CNT growth. Raman spectroscopy characterization indicates high quality CNTs grown by this approach. This technique provides an inexpensive and simple route for addition of catalyst for Fe-based surface growth of CNTs.

Introduction

Given their unique structure, size, and physical properties,[1,2] carbon nanotubes (CNTs) have been considered for a growing number of important applications. Interesting technological device performances have been reported in the form of CNT field emitters,[3,4] capacitors,[5,6] sensors,[7,8] field effect transistors (FET),[9,10] and molecular filters,[11,12] among others. Many of these applications have triggered the search for low cost and large scale CNT production processes, and these are now becoming a reality.[13] There are several reports in the literature focusing on the improvement of traditional CNT synthesis methods.[14] Chemical vapor deposition (CVD) has emerged as a promising technique for CNT growth, suitable for large areas (wafer-scale) and irregular substrates. In addition, thermal CVD growth is free from the complications of abundant uncontrollable radicals found in most common plasma-related growth techniques[15] and allows relatively simple control of crucial CNT growth parameters. Scale-up of CNT production, while maintaining simplicity in the growth process, has been a common goal of many research efforts. The search for a cost-effective production process has motivated investigation into alternative catalyst deposition methods,[16−19] multicomponent catalyst materials (besides Fe, Co, and Ni),[20,21] and new substrates and catalyst supports to aid and assist the growth process.[22,23]

One crucial aspect of CVD-grown CNTs is the requirement for external deposition of catalyst on a solid oxide surface prior to growth. There have been a wealth of studies documenting unique catalyst deposition techniques such as metal evaporation,[24] roll-to-roll metal and oxide support evaporation,[19]

[†] Department of Chemistry.
[‡] The Richard E. Smalley Institute for Nanoscale Science and Technology.
[§] Department of Physics and Astronomy.
[||] Department of Mechanical Engineering and Materials Science.

(1) Dresselhaus, M. S.; Dresselhaus, G.; Avouris, P. *Carbon Nanotubes Synthesis, Structure, Properties and Applications*; Springer-Verlag: Berlin, Germany, 2001.
(2) Saito, R.; Dresselhaus, G.; Dresselhaus, M. S. *Physical Properties of Carbon Nanotubes*; Imperial College Press: London, U.K., 1998.
(3) Jung, S. M.; Jung, H. Y.; Suh, J. S. *Carbon* **2008**, *46*, 1973–1977.
(4) Rakhi, R. B.; Sethupathi, K.; Ramaprabhu, S. *Carbon* **2008**, *46*, 1656–1663.
(5) Chou, S.; Wang, J.; Chew, S.; Liu, H.; Dou, S. *Electrochem. Commun.* **2008**, *10*, 1724–1727.
(6) Kimizuka, O.; Tanaike, O.; Yamashita, J.; Hiraoka, T.; Futaba, D. N.; Hata, K.; Mashida, K.; Suematsu, S.; Tamamitsu, K.; Saeki, S.; Yamada, Y.; Hatori, H. *Carbon* **2008**, *46*, 1999–2001.
(7) Kong, J.; Franklin, N. R.; Zhou, C.; Chapline, M. G.; Peng, S.; Cho, K.; Dai, H. *Science* **2000**, *287*, 622–625.
(8) Snow, E. S.; Perkins, F. K.; Houser, E. J.; Badescu, S. C.; Reinecke, T. L. *Science* **2005**, *307*, 1942–1945.
(9) Vaillancourt, J.; Lu, X.; Han, X.; Janzen, D. C.; Reinecke, T. L. *Elecron. Lett.* **2006**, *42*, 1365–1366.
(10) Javey, A.; Guo, J.; Farmer, D. B.; Wang, Q.; Yenilmez, E.; Gordon, R. G.; Lundstrom, M.; Dai, H. *Nano Lett.* **2004**, *4*, 1319–1322.
(11) Hinds, B. J.; Chopra, N.; Rantell, T.; Andrews, R.; Gavalas, V.; Bachas, L. G. *Science* **2004**, *303*, 62–65.
(12) Majumder, M.; Keis, K.; Zhan, X.; Meadows, C.; Cole, J.; Hinds, B. J. *J. Membr. Sci.* **2008**, *316*, 89–96.
(13) Service, R. F. *Science* **1998**, *281*, 940–942.
(14) Merchan-Merchan, W.; Saveliev, A. V.; Kennedy, L. A. *Carbon* **2004**, *42*, 599–608.
(15) Liu, C.; Chen, Y. C.; Tzeng, Y. *Diamond Relat. Mater.* **2004**, *13*, 1274–1280.
(16) Franklin, N. R.; Li, Y.; Chen, R. J.; Javey, A.; Dai, H. *Appl. Phys. Lett.* **2001**, *79*, 4571–4573.
(17) Murakami, Y.; Chiashi, S.; Miyauchi, Y.; Hu, M.; Ogura, M.; Okubo, T.; Maruyama, S. *Chem. Phys. Lett.* **2004**, *385*, 298–303.
(18) Méhn, D.; Fonseca, A.; Bister, G.; Nagy, J. B. *Chem. Phys. Lett.* **2004**, *393*, 378–384.
(19) Pint, C. L.; Pheasant, S. T.; Pasquali, M.; Coulter, K. E.; Schmidt, H. K.; Hauge, R. H. *Nano Lett.* **2008**, *8*, 1879–1883.
(20) Lima, M. D.; Jung de Andrade, M.; Locatteli, A.; Balzaretti, N.; Nobre, F.; Perez-Bergmann, C.; Roth, S *Phys. Status Solidi B* **2007**, *244*, 3901–3906.
(21) Jiang, Q.; Song, L. J.; Zhao, Y.; Lu, X. Y.; Zhu, X. T.; Qian, L.; Ren, X. M.; Cai, Y. D. *Mater. Lett.* **2007**, *61*, 2749–2752.
(22) Qingwen, L.; Hao, Y.; Yan, C.; Jin, Z.; Zhongfan, L. *J. Mater. Chem.* **2002**, *12*, 1179–1183.
(23) Gao, L. Z.; Kiwi-Minsker, L.; Renken, A. *Surf. Coat. Technol.* **2008**, *202*, 3029–3042.
(24) Nasibulin, A. G.; Moisala, A.; Brown, D. P.; Jiang, H.; Kauppinen, E. I. *Chem. Phys. Lett.* **2005**, *402*, 227–232.

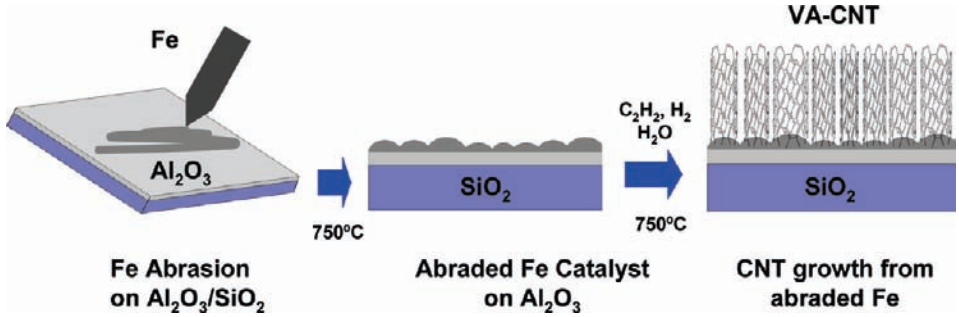

Figure 1. Scheme that describes catalyst deposition through abrasion. Any object with Fe metal content abrades catalyst in the form of particles that can be used as nucleation sites for CNT growth.

sputtering,[25] nanoparticle spin-coating,[16] dip-coating,[17] sol−gel,[18] and layer by layer metal deposition,[26] among others. All of these approaches support CNT growth, although some are more effective than others. In addition to catalyst deposition techniques, several studies have focused on different supporting substrates for CNT growth. The use of quartz and glass instead of Si/SiO_2 is quite common, and recent studies have emphasized that growth can be achieved on bulk metals, including stainless steel (SS) foils, where additional metal catalyst is not required.[27−29] Recently, CNT growth has been reported from grinding hardened steel balls with graphite, with mechanical milling followed by thermal annealing at 1400 °C.[30] In that study, milling times as long as 200 h were used to produce CNTs. In addition, Yuan et al. have recently reported CNT growth on quartz where the catalyst was deposited via scratching[31] in a manner similar to our observations. More recently, two research groups have reported metal-free CNT growth, through SiO_2 particles abraded upon a surface.[32−34] Another approach toward continuous CNT production involves the use of aluminum foil as the catalyst supporting surface, although this route still requires Fe catalyst deposition to achieve CNT growth.[35] Growing CNTs on metallic substrates or conductive substrates is essential for the development of CNT-based applications such as field emitters and other electronic devices, where good electrical contact between the CNTs and the metallic contacts is needed. Although there has been a reasonable level of success achieved along these lines, there still remains significant room for improvement of CNT properties, and simple catalyst deposition techniques that result in high yield and scalable growth of high quality CNTs are needed. To date, the water-assisted CVD supergrowth process remains the most efficient process for high yield, high-quality CNT growth in a dense aligned structure.[19,36−40]

In this study, we report abrasion as a simple, cost-effective deposition technique of catalyst that supports high density CNT growth and micro- and nanoscale patterning. Mechanical friction applied between a metal surface and the growth substrate abrades enough catalyst onto an oxide supporting layer to result in the growth of dense vertically aligned CNT forests (VA-CNTs) with a reasonably high quality compared to other processes for CNT synthesis. This work presents a new route toward catalyst deposition from easily obtained bulk materials, with the capability to impact cost-effectiveness of currently developing CNT applications.

Experimental Section

The catalyst deposition technique relies on simple mechanical friction generated between a solid metal catalyst source and a 10−100-nm-thick film of Al (forming Al_2O_3) deposited on a SiO_2 substrate. A number of different catalyst sources were used, including magnetic Fe, cast Fe, carbon steel, 99.98% pure Fe from Alfa Aesar, and SS series 300 (SS-302, SS-316) and 400 (SS-416, SS-420). The catalyst sources involved many different shapes and forms such as discs, blades, bars, granules, and wool fibers. By rubbing any Fe metal object against an Al_2O_3/SiO_2 substrate, catalytic Fe particles are transferred to the growth substrate, as shown in Figure 1. The pressure applied during the abrasion resulted in the deposition of a light to heavy coating of Fe particles on the substrate, depending on the conditions. At low pressures, CNTs were observed on the surface only as mats or sparsely grown domains. However, when greater pressure was applied, a higher concentration of catalyst particles was deposited on the growth substrate, resulting in the formation of a vertical array of CNTs.

CVD growth experiments were carried out in a hot filament chemical vapor deposition (HF-CVD) apparatus, which has been described elsewhere.[19,41,42] To chemically reduce the deposited metal and produce an active catalyst, after rapid insertion of the abraded substrate into a hot furnace, a brief exposure to atomic hydrogen produced via a hot tungsten filament preceded the growth process. A total flow rate of ∼400 standard cubic centimeters per

(25) Delzeit, L.; Chen, B.; Cassell, A.; Stevens, R.; Meyyappan, M. *Chem. Phys. Lett.* **2001**, *348*, 368–374.
(26) Liu, J.; Li, X.; Schrand, A.; Ohashi, T.; Dai, L. *Chem. Mater.* **2005**, *17*, 6599–6604.
(27) Baddour, C. E.; Fadlallah, F.; Nasuhoglu, D.; Mitra, R.; Vandsburger, L.; Meunier, J.-L. *Carbon* **2008**, *47*, 313–317.
(28) Karwa, M.; Iqbal, Z.; Mitra, S. *Carbon* **2006**, *44*, 1235–1242.
(29) Park, D.; Kim, Y. H.; Lee, J. K. *J. Mater. Sci.* **2003**, *38*, 4933–4939.
(30) Chen, Y.; Conway, M. J.; Fitzgerald, J. D. *Appl. Phys. A: Mater. Sci. Process.* **2003**, *76*, 633–636.
(31) Yuan, D.; Ding, L.; Chu, H.; Feng, Y.; McNicholas, T. P.; Liu, J. *Nano Lett.* **2008**, *8*, 2576–2579.
(32) Liu, B.; Ren, R.; Gao, L.; Li, S.; Pei, S.; Liu, C.; Jiang, C.; Cheng, H. M. *J. Am. Chem. Soc.* **2009**, *131*, 2082–2083.
(33) Huang, S.; Cai, Q.; Chen, J.; Qian, Y.; Zhang, L. *J. Am. Chem. Soc.* **2009**, *131*, 2094–2095.
(34) Hirsch, A. *Angew. Chem., Int. Ed.* **2009**, *48*, 5403–5405.
(35) Yoshikawa, N.; Asari, T.; Kishi, N.; Hayashi, S.; Sugai, T.; Shinohara, H. *Nanotechnology* **2008**, *19*, 245607(5).
(36) Hata, K.; Futaba, D. N.; Mizuno, K.; Namai, T.; Yumura, M.; Iijima, I. *Science* **2004**, *306*, 1362–1364.
(37) Nishino, H.; Yasuda, S.; Namai, T.; Futaba, D. N.; Yamada, T.; Yumura, M.; Iijima, S.; Hata, K. *J. Phys. Chem. C* **2007**, *111*, 17961–17965.
(38) Xu, Y.; Flor, E.; Kim, M. J.; Hamadani, B.; Schmidt, H.; Smalley, R. E.; Hauge, R. H. *J. Am. Chem. Soc.* **2006**, *128*, 6560–6561.
(39) Gong, K.; Chakrabarti, S.; Dai, L. *Angew. Chem., Int. Ed.* **2008**, *47*, 5446–5450.
(40) Chakrabarti, S.; Gong, K.; Dai, L. *J. Phys. Chem. C* **2008**, *112*, 8136–8139.
(41) Pint, C. L.; Nicholas, N.; Pheasant, S. T.; Duque, J. G.; Parra-Vasquez, A. N. G.; Eres, G.; Pasquali, M.; Hauge, R. H. *J. Phys. Chem. C* **2008**, *112*, 14041–14051.
(42) Pint, C. L.; Pheasant, S. T.; Parra-Vasquez, A. N. G.; Horton, C.; Xu, Y.; Hauge, R. H. *J. Phys. Chem. C* **2009**, *113*, 4125–4133.

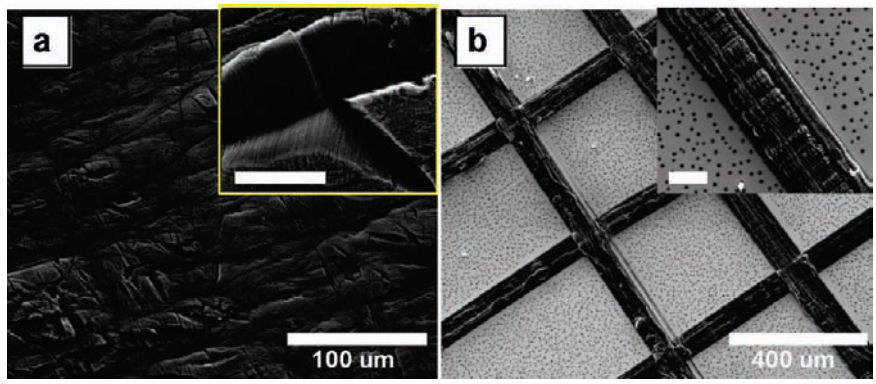

Figure 2. SEM images of (a) a top-down view of a dense CNT forest and (b) a top-down view of microscale patterned CNTs, both formed from abrasion of Fe (SS-420) catalyst through abrasion. Inset images show higher resolution images of (a) the CNT alignment in the dense array and (b) a single line formed from abrasion. Scale bars in inset images are 20 μm.

min (sccm) of H_2, 2 sccm H_2O, and 2 sccm C_2H_2 was maintained in the 1 in. tube furnace under 1.4 Torr vacuum while the abraded substrate was introduced and CNTs were grown. The temperature was maintained at 750 °C for the duration of the process, settings that have been found to yield the highest quality growth in water-assisted conditions.[42]

Alumina coated substrates, with 100-nm-thick Al_2O_3 deposited through atomic layer deposition (ALD) of Al onto a clean SiO_2 wafer, were provided by Sundew Technologies LLC. A 10-nm-thick Al_2O_3 layer was prepared by electron beam evaporation of Al at typical pressures of 10^{-6} Torr.

Results and Discussion

SS has been previously simultaneously used both as the catalyst source and the substrate[27−29,43,44] for CNT growth. Other processes require additional Fe to be deposited on the SS substrates[45−47] to achieve CNT growth. The results here indicate that all the Fe-containing alloys abraded on Al_2O_3 grow CNTs, once deposited on a proper supporting substrate, although some Fe-containing sources appear more efficient than others. Figure 2a shows VA-CNTs grown on Al_2O_3 substrates as a dense forest while Figure 2b shows micrometer-wide patterns of CNTs where SS-420 was abraded through single stripes made by a sharp scalpel. As shown in Figure 2b, patterns of dense, aligned CNTs can be easily obtained in this technique with a feature resolution determined by the size of the object used for abrasion. We also note that some Fe sources abrade more easily than others. The SS-420 hardness on the Hardness Brinell (HB) scale is higher than that of SS-316; however, abrasion occurs more easily with SS-420. This is probably related to the machinability of SS-420 compared to SS-316; SS-316 machinability rates are lower and cause higher tool wear than SS-420. SS has many potential active components for CNT growth, including Fe and Ni, both of which are known as catalysts for CNT growth.[48] However, the SS-400 series (SS-416 and SS-420) has no Ni in the SS matrix but still results in the growth of VA-CNTs. This suggests that Ni is not a required component in the growth process and allows us to focus on Fe as the likely active component of CNT growth. In addition, Cr and C content appear to have some effect on the abrasion process. The presence of Cr presumably results in surface hardness enhancement of SS that affects the Fe transfer through abrasion. The presence of carbon in the SS also increases hardness and might accelerate the nucleation and growth of CNTs.

To study the properties of the CNT arrays grown from abraded catalyst, data from Raman spectroscopy (laser excitation at 514, 633, and 785 nm) was collected and is shown in Figure 3a. In all spectra, the D/G ratio remains small, indicative of the low-defect CNT growth that is characteristic of the water-assisted CVD process. The low D/G ratios are comparable to those from VA-CNTs grown in the water-assisted CVD process from e-beam evaporated catalyst sources.[38,49] Raman spectra of CNTs in the solid state and CNTs dispersed in sodium dodecyl benzene sulfonate (SDBS) surfactant show no significant D/G ratio difference. The radial breathing modes (RBM) in Figure 3a indicate the presence of CNTs with walls less than $\sim$2 nm in diameter, which can be due to the inner walls of multiwalled carbon nanotubes (MWCNTs) or small diameter single-walled carbon nanotubes (SWCNTs).[50] Figure 3b shows an atomic force microscope (AFM) image of particles deposited in a single stripe abrasion with a SS scalpel. A large particle size distribution was found, including many particles larger than 10 nm. The diameter range of VA-CNTs grown from these particles suggests that it may not be necessary to have small diameter (<10 nm) particles present to sustain uniform nucleation and growth of VA-CNTs. Transmission electron microscope (TEM) images (Figure 4a) obtained after dispersing the CNTs through 15 min of bath sonication in ethanol and deposition on lacey carbon TEM grids suggest the presence of a variety of CNT species, including SWCNTs, double-walled CNTs, and MWCNTs. When dispersed in SDBS with 6 h of bath sonication, the CNTs display fluorescence, albeit weak, with excitation at 660 nm, indicating the presence of small amounts of semiconducting SWCNT species.[51]

Comparison of XPS spectra of the catalysts deposited by abrasion and e-beam evaporation provides further support for the presence Fe on abraded substrates. XPS analysis indicates that Fe deposited through abrasion has features

(43) Zhou, Q.; Li, C.; Gu, F.; Du, H. L. *J. Alloys Compd.* **2008**, *463*, 317–322.
(44) Wang, N.; Yao, B. D. *Appl. Phys. Lett.* **2001**, *78*, 4028–4030.
(45) Masarapu, C.; Wei, B. *Langmuir* **2007**, *23*, 9046–9049.
(46) Talapatra, S.; Kar, S.; Pal, S. K.; Vajtai, R.; Ci, L.; Victor, P.; Shaijumon, M. M.; Kaur, S.; Nalamasu, O.; Ajayan, P. M. *Nat. Nanotechnol.* **2006**, *1*, 112–116.
(47) Hiraoka, T.; Yamada, T.; Hata, K.; Futaba, D. N.; Kurachi, H.; Uemura, S.; Yumura, M.; Iijima, S. *J. Am. Chem. Soc.* **2006**, *128*, 13338–13339.
(48) Kuang, M. H.; Wanga, Z. L.; Bai, X. D.; Guo, J. D.; Wanga, E. G. *Appl. Phys. Lett.* **2000**, *76*, 1255–1257.
(49) Pint, C. L.; Xu, Y.; Pasquali, M.; Hauge, R. H. *ACS Nano* **2008**, *2*, 1871–1878.
(50) Dresselhaus, M. S.; Dresselhaus, G.; Saito, R.; Jorio, A. *Phys. Rep.* **2005**, *409*, 47–99.
(51) Bachilo, S. M.; Strano, M. S.; Kittrell, C.; Hauge, R. H.; Smalley, R. E.; Weisman, R. B. *Science* **2002**, *298*, 2361–2366.

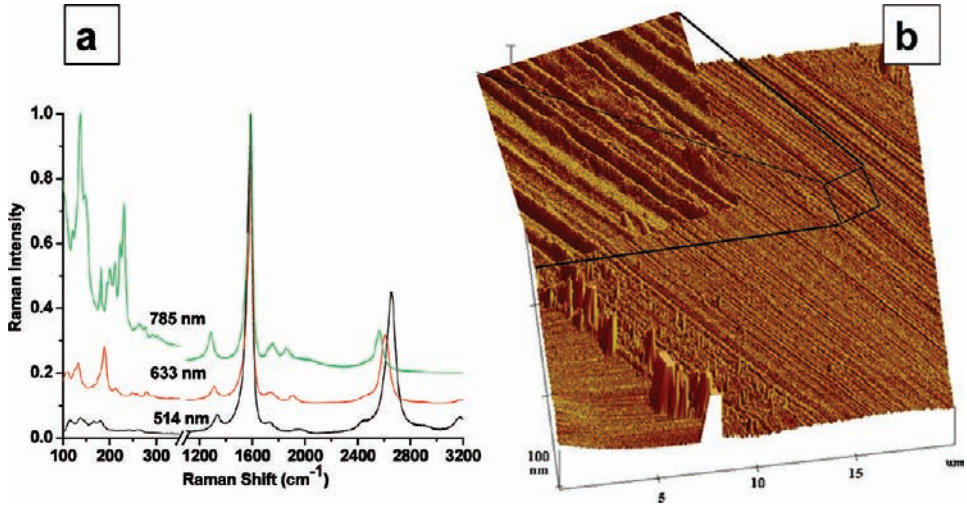

Figure 3. (a) Raman spectra at three excitation wavelengths from a typical dense forest of VA-CNTs grown from Fe catalyst (surgical scalpel SS-420) deposited through abrasion on an Al_2O_3 supporting surface. (b) AFM image of single stripes drawn with a surgical scalpel (SS-420) on an Al_2O_3 substrate before CNT growth, revealing the particles that form during abrasion and that support the VA-CNT growth. The image is 20 μm on a side while the inset is 1 μm on a side collected from the area in the square.

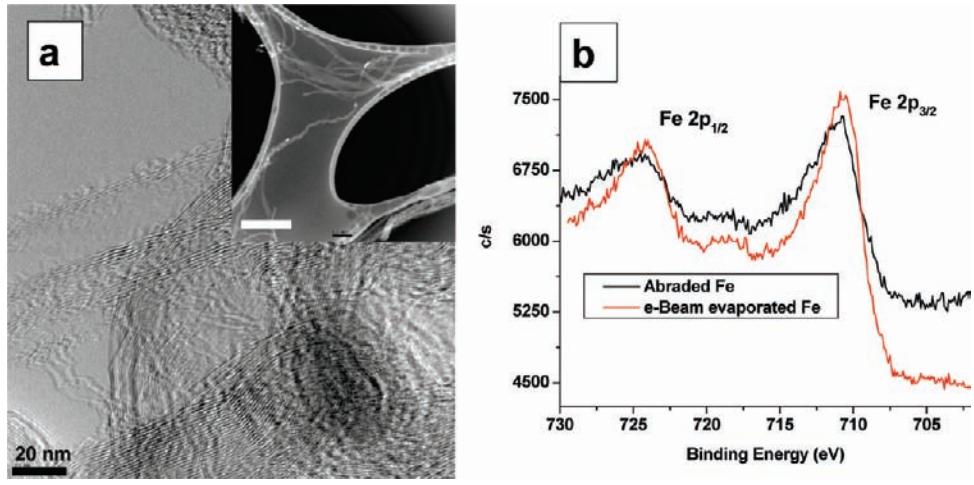

Figure 4. TEM images of CNTs from a typical dense forest of VA-CNTs grown from abrasion deposited catalyst (surgical scalpel SS-420) on an Al_2O_3 film. The CNTs were removed by sonication and dispersed in ethanol and applied to a lacy carbon grid for imaging (a), inset image scale bar is 200 nm. Fe content comparison by XPS spectra between catalyst deposited through abrasion and e-beam evaporation on Al_2O_3 substrates (as prepared).

similar to a 1 nm Fe layer deposited by e-beam evaporation (Figure 4b), the latter being the most common catalyst layer used in VA-CNT growth.[19,52,53] In addition, SEM images of a surgical scalpel (SS 420) used as a catalyst source before and after metal abrasion reveals the removal of some material from the initial scalpel (see Supporting Information Figure S1). To demonstrate that this approach is applicable to larger areas, the scalpel was used to abrade upon a rotating substrate (~3000 rpm), quickly generating circular patterns of catalyst on ~1 cm diameter substrates in an open environment, as shown in Figure 5a. Furthermore, exposure to water-assisted growth conditions resulted in VA-CNT growth with circular patterns as shown in Figure 5b.

In addition to using abrasion geared toward large-scale production of VA-CNTs or forming microscale patterns of VA-CNTs, the use of abrasion for the formation of nanoscale patterns has been explored. A 12-nm-layer of Fe was e-beam deposited onto a conventional silicon AFM tip. Using contact mode AFM, catalyst patterns were drawn. Figure 6 is a patterned catalyst stripe having a length of ~5 μm on ALD-deposited alumina substrates. Prior to deposition of the Fe, the AFM tip diameter was ~20 nm; after Fe deposition the diameter was ~40 nm. Therefore the resolution of the Fe pattern obtained is limited by the radius of curvature of the tip, similar to the process described in Figure 2. To demonstrate this, Fe was deposited using 2, 5, and 10 AFM scans, as shown in Figure 6a (10 scans). Following catalyst deposition, the catalyst stripe was exposed to water-assisted CVD growth conditions, which resulted in the growth of a significant number of CNTs, as shown in Figure 6b. The height of the deposited catalyst was typically found to be 1−3 nm, although some larger particles (10−20 nm) at the edges of the pattern were observed. As expected, the amount of catalyst deposited decreased with the number of scans. However, it should be noted that this catalyst deposition process can be just as easily carried out with used or broken AFM tips, decreasing the cost of the nanoscale

(52) Pint, C. L.; Bozzolo, G.; Hauge, R. H. *Nanotechnology* **2008**, *19*, 405704(11).
(53) Wei, Y. Y.; Eres, G.; Merkulov, V. I.; Lowndes, D. H. *Appl. Phys. Lett.* **2001**, *78*, 1394–1396.

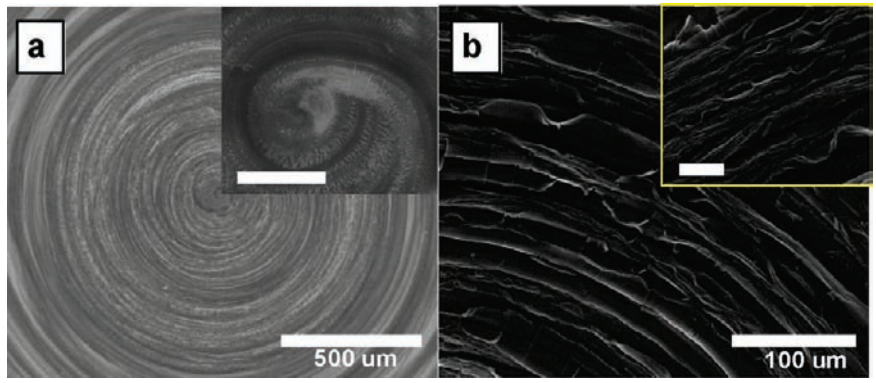

Figure 5. SEM images of (a) abraded Fe (SS-420 surgical scalpel) deposited on a spinning Al_2O_3 substrate. (b) SEM images of CNTs grown from catalyst deposited through abrasion on a spinning Al_2O_3 substrate. Scale bars in the inset images are 25 μm.

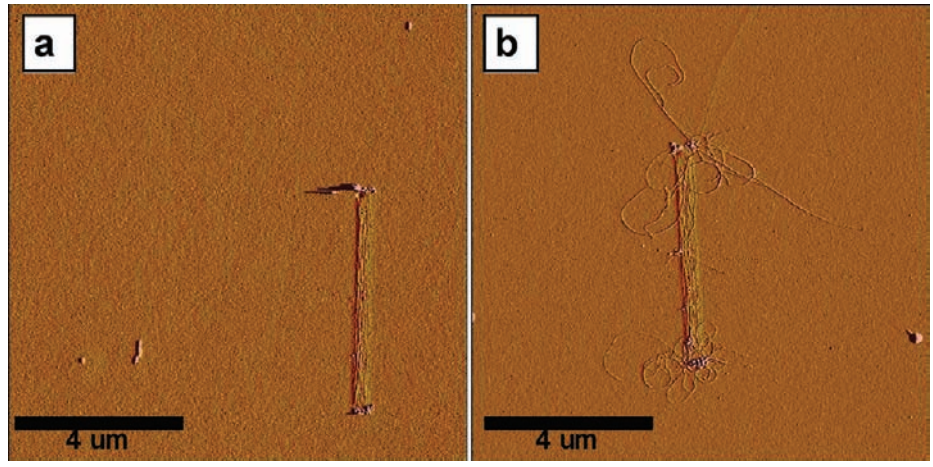

Figure 6. (a) AFM image of catalyst patterns drawn from abrasion using an AFM tip coated with a thin layer of evaporated Fe metal. (b) CNTs grown from a nanopatterned catalyst drawn with the Fe-coated AFM tip.

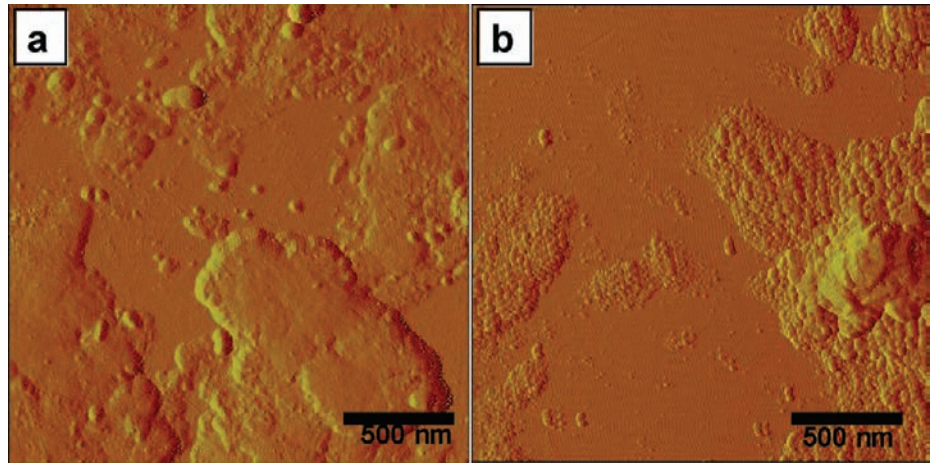

Figure 7. AFM images of abraded Fe on Al_2O_3: (a) before and (b) after heating to 750 °C for 60 s in a typical CNT growth environment (H_2/H_2O). After heating, the surface of the catalyst particles has developed into a "nano-dome" morphology that supports CNT nucleation and growth.

patterning. Ideally, a standard contact mode AFM tip should be used, although the radius of curvature of the tip would be larger, which would affect the width of the patterns.

There are additional advantages to the abrasion catalyst deposition method. It is generally accepted that catalyst particle size determines the diameter of the CNT.[37,54] As is evident from the AFM images of particles deposited through abrasion (Figure 7a), the majority of deposited particles are much larger than that expected to grow CNTs of diameters and quality shown in Figures 3 and 4. In conventional VA-CNT growth substrates, the catalyst film thickness is generally the factor which determines the size of islands that nucleate CNTs.[53] Among others, Wei et al.[53] have reported that a minimal catalyst thickness is required to successfully grow VA-CNT. The fact that dense, uniform CNT growth is observed on a full 1 cm^2

(54) Cheung, C. L.; Kurtz, A.; Park, H.; Lieber, C. M. *J. Phys. Chem. B* **2002**, *106*, 2429–2433.

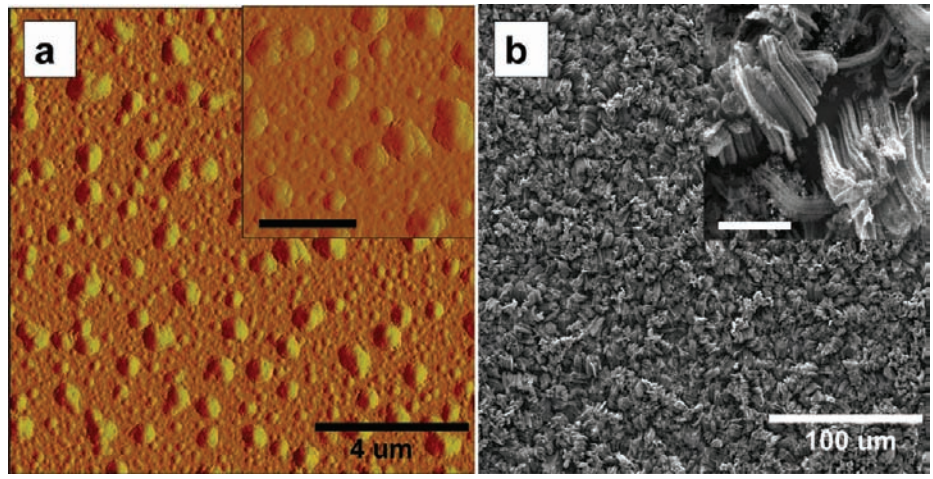

Figure 8. Controlled catalyst deposition through abrasion using 100 mesh SS particles in a vortex agitator. (a) As deposited catalyst, inset image scale bar is 2 μm. (b) CNTs grown from Fe deposited through a vortex system abrasion, inset image scale bar is 10 μm.

substrate is interesting in the framework of understanding CNT growth from nanoscale particles. From the AFM images of Figure 7a, it is evident that these larger Fe particles exposed at 750 °C for 60 s results in the formation of smaller semispherical particles as shown in Figure 7b. It is generally observed that nanoparticles larger than a typical CNT diameter initially have smoother and flatter surfaces (Figure 7a), which changes in the early stage of CNT growth, as soon as they are exposed to reduction conditions at 750 °C. At this temperature under reduction conditions, dome-like structures emerge with feature sizes generally corresponding to the range of CNT diameters observed (Figure 7b). This indicates that these "nano-dome" features are the precursors for nucleation and subsequent CNT growth.

Several mechanisms for CNT growth have been proposed in the literature; however, the process is not fully understood. The most accepted mechanisms are bulk carbon diffusion and precipitation, surface migration, and carbide formation.[55] In a similar manner to particle size changes reported by Park et al.,[29] Zhou et al.,[43] and Gao et al.,[23] we have observed a large number of nanometer-sized particles forming on SS substrates when exposed at 750 °C for 15 min under C_2H_2, H_2, and H_2O flow. Under these typical CNT growth conditions, bulk SS substrates develop cracks and particle formation as a result of sintering, leaving a different surface morphology than the original one, with only a few fibrillar or MWCNTs observed during growth (no VA-CNTs). This is evidence of C diffusion into the substrate, but since diffusion is continuous through the bulk Fe metal, the concentration of C is not high enough to promote CNT nucleation. This observation suggests that C diffusion followed by saturation and precipitation are important steps for CNT growth.[56] A SS-420 scalpel that had been previously heat-treated in a growth environment was used for catalyst abrasion on a new Al_2O_3 substrate. This C rich SS was quite easily abraded on Al_2O_3 substrates and promoted good CNT growth with denser and longer CNTs. This observation is similar to results reported by Liu et al.,[15] where sputter-cast Fe gave better growth than pure Fe, suggesting that preabsorbed C in the catalyst promotes faster CNT nucleation.

Although abrasion is a simple and effective technique for catalyst deposition, the application of manual force to generate abrasion leads to difficulty in reproducing specific conditions of the abrasion process. To study this process quantitatively, a controlled mechanical device was developed to enhance reproducibility in consecutive experiments. This was achieved with the use of a vortex agitator having a fixed substrate on the bottom surface held via double-sided adhesive tape. The substrate was covered with ~10 g of Fe source, granules, SS-420 powder, SS-420 balls, or steel wool, and agitated for different periods of time resulting in a more controlled abrasion of the Fe onto the substrate. This setup allowed control of the variable parameters time, speed, and power intensity of the vortex, which provides better control of the pressure and abrasion forces between the particles and substrate. Initial studies indicate a more homogeneous distribution of catalyst transferred over the entire substrate. Formations of island-like patches of transferred catalyst have been observed (Figure 8a) that support the nucleation and growth of dense CNTs (Figure 8b). This process can be used for uniform, large-area coating of catalyst layers that support dense CNT growth.

It is not clear whether the abrasion process results in a catalyst that is strongly or weakly adhered to the substrate. To better determine this, the catalyst-abraded substrate was washed with ethanol, and the rinse was applied onto a different, clean Al_2O_3 substrate. Both the abraded and the rinse-exposed substrates were then subjected to the CNT growth conditions and both exhibited CNT growth. In the first case, the substrate on which abrasion was carried out grew patches of CNTs, indicating that much of the abraded metal was firmly attached to the Al_2O_3 surface. However, the growth observed on the second substrate (from the dried ethanol rinse) typically occurred from small flakes of alumina containing abraded metal that had lodged on the surface and grew microfibrillar, dense CNTs as shown in Figure 9. It should be noted that this growth process was similar to "flying carpet" growth,[19] with some of the catalyst-coated flakes growing away from the substrate (Figure 9a) or growing CNT fibrils from the substrate (Figure 9b) based upon the orientation of the catalyst on the flake with respect to the supporting surface.

In addition to catalyst deposition, dense aligned CNT growth by CVD requires the presence of a thin supporting oxide layer

(55) Rodriguez-Manzo, J. A.; Terrones, M.; Terrones, H.; Kroto, H. W.; Sun, L.; Banhart, F. *Nat. Nanotechnol.* **2007**, *2*, 307–311.
(56) Deck, C. P.; Vecchio, K. *Carbon* **2006**, *44*, 267–275.

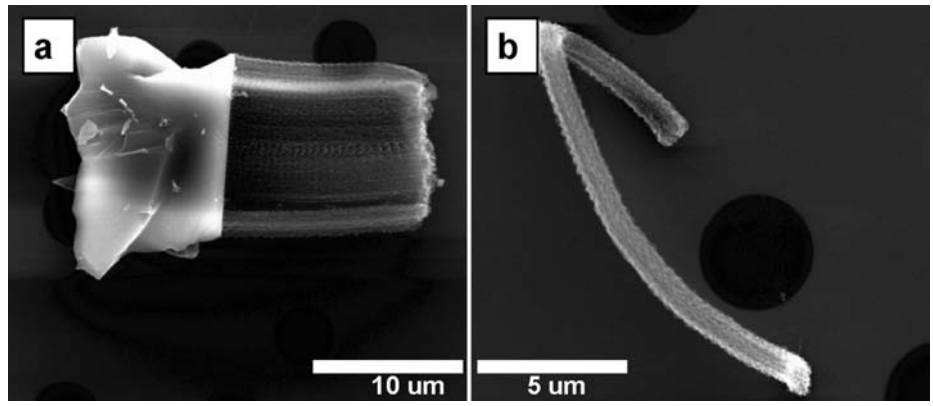

Figure 9. SEM images of CNT grown from surgical scalpel (SS-420)-treated Al_2O_3 flakes that had been transferred through rinsing to a second substrate before CNT growth. (a) VA-CNTs with an Al_2O_3 flake attached on the base of the array and (b) a rope of CNTs without an observed Al_2O_3 flake or support.

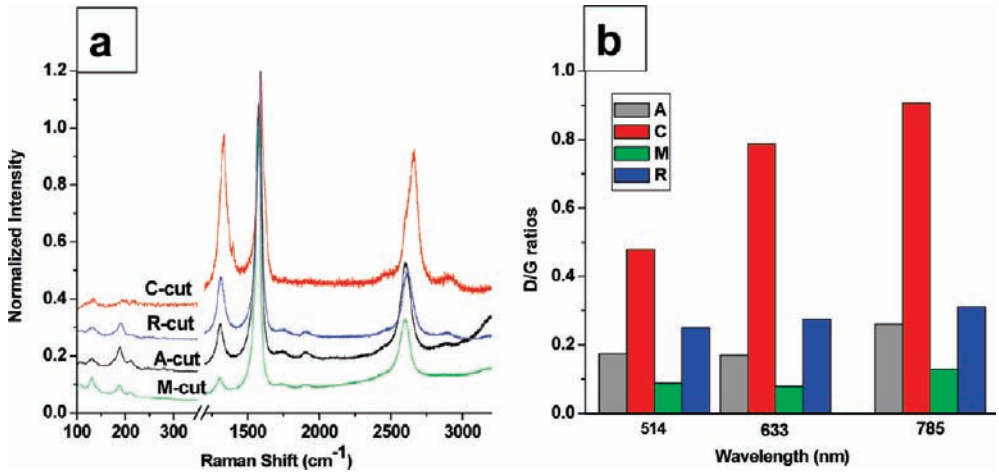

Figure 10. Raman spectra of CNT grown from abraded Fe (surgical scalpel SS-420) on A, C, M, and R single crystal cuts of Al_2O_3 substrates. (a) Spectra showing both the RBM region and D and G bands for CNTs grown on the different cuts and (b) D/G ratios for all cuts at the three different laser excitation energies utilized.

(Al_2O_3) to support the metal catalyst. In the processes described thus far, an e-beam deposited Al_2O_3 layer (from Al) was used to support the abraded catalyst. We also abraded an Al_2O_3 layer onto the SiO_2 through the abrasion of Al onto a Si/SiO_2 wafer followed by Fe abrasion. Although Al abrasion can be simply achieved, the planarity and smoothness of the surface that enhances the uniform abrasion of Fe was lost. As a result, CNT growth on these substrates no longer produced a continuous dense forest over the whole surface. Second, we investigated the use of a bulk alumina substrate (not atop Si/SiO_2) wherein the direct abrasion of catalyst onto the bulk Al_2O_3 surface was performed. In general, it was observed that this process does promote the growth of dense CNTs but is complicated by the enhanced surface roughness of Al_2O_3 discs and other inexpensive forms of Al_2O_3. The root-mean-square (rms) roughness of a typical polycrystalline, unpolished, bulk alumina substrate is on the order of micrometers, while the rms roughness of a typical ALD-deposited Al_2O_3 layer is less than 0.25 nm. The low rms roughness appears to be important for the abrasion process to yield catalyst layers that will support the growth of uniform, dense CNT arrays. To study the abrasion process on bulk Al_2O_3 materials, we used single crystals of Al_2O_3 that were epitaxially polished. This leads to smooth surfaces that allow the abrasion of Fe similar to that observed for the e-beam or ALD deposited Al_2O_3 layers. Fe abraded on the single crystal substrates grows uniform, dense aligned carbon nanotubes over the entire abraded surface, except for one. For the different A, C, M, and R crystals, only the C-cut exhibited poor growth. Analysis of the RBMs of the resulting CNTs shows a variety of SWCNT diameters but only slight differences between growth on the different crystal cuts. However, distinct differences arise when comparing the D and G bands (Figure 10), as the D/G ratio appears smaller for CNTs grown on A, M, and R cuts. Interestingly, the D/G ratio is consistently large for the growth that occurs from the C-cut Al_2O_3 that demonstrated poor growth. Since the rms surface roughnesses of all four surfaces are not substantially different, there may be a fundamental difference in the efficiency of a catalyst supported on a C-cut Al_2O_3 surface compared to the other faces, even though there is no obvious reason why the catalyst deposition process should be different on the various surfaces. Nonetheless, catalyst deposition for uniform and high quality CNT growth can be achieved on smooth bulk Al_2O_3 surfaces, which further illuminates the capability and utility of the abrasion process for catalyst deposition.

Conclusions

A simple approach for catalyst deposition on substrates at ambient conditions based upon mechanical abrasion of inexpensive bulk metals onto catalyst supports has been demonstrated. This technique can be used to make micrometer-scale and

even nanoscale patterned surfaces of dense CNTs, in addition to providing a useful approach to large-scale catalyst deposition. The microscopic morphology of the film is important as well as the nucleation behavior of the catalyst particles. Finally, growth results for abrasion catalyst deposition on single crystal cuts of Al_2O_3 suggest that A, M, and R faces are better than the C-cut for catalyst abrasion that supports dense CNT growth.

Acknowledgment. The authors thank Sundew Technologies LLC, Bromfield, CO, for providing ALD coated Al_2O_3 substrates and Carter Kittrell for helpful discussions. This work was supported by the Air Force Laboratories under Contract Number FA8650-05-D-5807, Materials Science and Engineering, Oak Ridge National Laboratory, Department of Energy (subcontract DE-4000064987).

Supporting Information Available: SEM images of the surgical scalpel before and after abrasion. This material is available free of charge via the Internet at http://pubs.acs.org.

JA905681A